

Mixed-Spectrum Signals – Discrete Approximations and Variance Expressions for Covariance Estimates

Filip Elvander and Johan Karlsson

Abstract—The estimation of the covariance function of a stochastic process, or signal, is of integral importance for a multitude of signal processing applications. In this work, we derive closed-form expressions for the variance of covariance estimates for mixed-spectrum signals, i.e., spectra containing both absolutely continuous and singular parts. The results cover both finite-sample and asymptotic regimes, allowing for assessing the exact speed of convergence of estimates to their expectations, as well as their limiting behavior. As is shown, such covariance estimates may converge even for non-ergodic processes. Furthermore, we consider approximating signals with arbitrary spectral densities by sequences of singular spectrum, i.e., sinusoidal, processes, and derive the limiting behavior of covariance estimates as both the sample size and the number of sinusoidal components tend to infinity. We show that the asymptotic regime variance can be described by a time-frequency resolution product, with dramatically different behavior depending on how the sinusoidal approximation is constructed. In a few numerical examples we illustrate the theory and the corresponding implications for direction of arrival estimation.

Keywords Array processing, covariance estimation, spectral analysis

I. INTRODUCTION

Modeling signals that impinge on sensor arrays appear in a large variety of signal processing applications, including radar, sonar, and audio signal processing [1]–[3]. Commonly in such applications, one seeks a spatial spectrum, describing the distribution of signal energy over the space of interest, e.g., azimuth and elevation in direction of arrival (DoA) estimation [4], allowing for localizing and tracking targets [5], [6] or for performing spatial filtering of the sensor signals [7]. In practice, the spatial spectrum is often inferred from the array covariance matrix as in, e.g., optimal filtering such as the Capon method [8], subspace methods as ESPRIT and MUSIC [9], [10], as well as more recent contributions exploiting sparse representations [11] as well as knowledge of underlying dynamics [6].

Commonly, it is assumed that the impinging signals are narrowband, or that they may be decomposed into narrowband components through filtering or by the use of short time Fourier transforms [12], and that time delays may be described as phase shifts of the source signal waveform [13]. Assuming that the impinging signals are uncorrelated, this then induces a low-rank structure in the array covariance matrix, which is exploited in estimation of the spatial spectrum, e.g., using the

Caratheodory-Fejer theorem for Toeplitz matrices in the case of uniform linear arrays [5], [14]. The success of covariance based approaches are thus dependent on the availability of accurate estimates of the array covariance matrix, and, in particular, on the speed of convergence of finite-sample estimators to their expectation. Typically it is assumed that a large number of independent samples are available for estimating the covariance [15]–[17]. However, the narrowband assumption would imply that the samples are highly correlated also over large time horizons. In particular, perfectly narrowband signals, i.e., signals whose spectra have support of measure zero, are not ergodic and exhibit no mixing. In practice, the signals may be band-limited but with non-zero bandwidth, and a relevant question is then how the spectral properties affect the accuracy of the covariance estimates for this class of signals. For signals decomposable as a finite sum of fixed amplitude sinusoids and a moving average process, the asymptotic normality of the array sample covariance matrix was proved in [18], with the asymptotic performance of frequency estimation algorithms being presented in [19], [20]. However, to the best of the authors' knowledge, no finite-sample results for the accuracy of covariance estimates for signals with general spectra exist in the signal processing literature. In particular, there are no widely available results on the dependence of finite-sample accuracy on the impinging signals' spectra.

In this work, we consider the problem of covariance estimation for signals with mixed spectra, consisting of a Gaussian part with a spectral density and a singular part. Specifically, we derive closed form expressions for the finite-sample variance of the covariance estimates, allowing for exactly quantifying the speed of convergence for estimates to their expected values. As is shown, the properties of the covariance estimates vary considerably depending on whether the singular parts of the spectrum are modeled by sinusoidal components with fixed or Gaussian amplitudes. Furthermore, for Gaussian processes with arbitrary spectral densities, we consider utilizing sinusoidal components for constructing singular spectrum approximations. For both fixed and Gaussian amplitudes, we show that these approximations converge in distribution to the target process as the spacing of frequency grid goes to zero. When estimating covariances from such a signal, a relevant limit is when both the time interval and the number of sinusoidal component in the approximation tends to infinity. We give explicit expression for the asymptotic variance for this case and note that the variance is a function of the product of the time window and the frequency resolution. As we show, the covariance estimates for the fixed amplitude and Gaussian amplitude approximations have variances that are upper and

F. Elvander is with the Stadius Center for Dynamical Systems, Signal Processing and Data Analytics, KU Leuven, 3001 Leuven, Belgium, (email: firstname.lastname@esat.kuleuven.be).

J. Karlsson is with the Department of Mathematics, KTH Royal Institute of Technology, Stockholm, Sweden (email: firstname.lastname@math.kth.se).

lower bounded, respectively, by that of the target process. In particular, this implies that evaluating, e.g., direction of arrival estimators that make use of second-order moments based on data simulated from such sinusoidal approximations may yield results that are not representative for such estimators' performance on data generated by processes with spectral densities. We derive conditions for when such singular approximations perfectly mimic the target process, thereby allowing for implementing any array processing scenario with arbitrary spectra.

II. SIGNAL MODEL

Consider two scalar wide-sense stationary (WSS) zero-mean complex circularly symmetric stochastic processes x and y on the real line with power spectra $d\mu_x$ and $d\mu_y$, and cross spectrum $d\mu_{xy}$. The covariance functions are the Fourier transform of the spectra, and thus given by

$$\begin{aligned} r_x(\tau) &\triangleq \mathbb{E} \left(x(t) \overline{x(t-\tau)} \right) = \int_{-\infty}^{\infty} e^{i2\pi\theta\tau} d\mu_x(\theta) \\ r_y(\tau) &\triangleq \mathbb{E} \left(y(t) \overline{y(t-\tau)} \right) = \int_{-\infty}^{\infty} e^{i2\pi\theta\tau} d\mu_y(\theta), \\ r_{xy}(\tau) &\triangleq \mathbb{E} \left(x(t) \overline{y(t-\tau)} \right) = \int_{-\infty}^{\infty} e^{i2\pi\theta\tau} d\mu_{xy}(\theta), \end{aligned} \quad (1)$$

for $\tau \in \mathbb{R}$, where \overline{z} denotes the complex conjugate of a complex scalar z , and $\mathbb{E}(\cdot)$ denotes the expectation operator. In this paper we focus on band-limited signals, and we will assume that all power spectra are supported in the frequency interval $\mathcal{I}_B = [\theta_c - B/2, \theta_c + B/2]$ and given by

$$d\mu_x(\theta) = \Phi_x(\theta)d\theta + \sum_{k=1}^{N_x} \alpha_k^2 \delta_{\theta_k^x}(\theta) \quad (2a)$$

$$d\mu_y(\theta) = \Phi_y(\theta)d\theta + \sum_{k=1}^{N_y} \beta_k^2 \delta_{\theta_k^y}(\theta), \quad (2b)$$

$$d\mu_{xy}(\theta) = \Phi_{xy}(\theta)d\theta. \quad (2c)$$

Here Φ_x , Φ_y , and Φ_{xy} are densities in $L_1(\mathcal{I}_B)$, α_k and β_k are positive constants, and $\delta_{\theta_k}(\theta) \triangleq \delta(\theta - \theta_k)$ where δ denotes the Dirac delta function.¹ Note that θ_c is the center frequency and B is the bandwidth of the signals.

Herein, we will consider two different models for x and y consistent with (2). Firstly, we consider a model where the sinusoidal components have random complex Gaussian amplitudes and thus also random initial phase, i.e.,

$$x(t) = x_a(t) + x_s(t) = x_a(t) + \sum_{k=1}^{N_x} a_k e^{i2\pi\theta_k^x t} \quad (3a)$$

$$y(t) = y_a(t) + y_s(t) = y_a(t) + \sum_{k=1}^{N_y} b_k e^{i2\pi\theta_k^y t} \quad (3b)$$

where x_a and y_a are Gaussian, band-limited, zero-mean random processes with absolutely continuous (cross)spectra Φ_x , Φ_y , Φ_{xy} , and where $a_k \sim \mathcal{CN}(0, \alpha_k^2)$ and $b_k \sim \mathcal{CN}(0, \beta_k^2)$

are complex Gaussian random variables. Secondly, consider the representation

$$x(t) = x_a(t) + x_s(t) = x_a(t) + \sum_{k=1}^{N_x} \alpha_k e^{i2\pi\theta_k^x t + i\varphi_k^x}, \quad (4a)$$

$$y(t) = y_a(t) + y_s(t) = y_a(t) + \sum_{k=1}^{N_y} \beta_k e^{i2\pi\theta_k^y t + i\varphi_k^y}, \quad (4b)$$

for $t \in \mathbb{R}$, where φ_k^x are independent random variables with uniform distribution $U((-\pi, \pi])$ (cf. [21]). For the covariance functions in (1), consider the standard estimates

$$\hat{r}_x(\tau; T) = \frac{1}{T} \int_{t=0}^T x(t) \overline{x(t-\tau)} dt, \quad (5a)$$

$$\hat{r}_y(\tau; T) = \frac{1}{T} \int_{t=0}^T y(t) \overline{y(t-\tau)} dt, \quad (5b)$$

$$\hat{r}_{xy}(\tau; T) = \frac{1}{T} \int_{t=0}^T x(t) \overline{y(t-\tau)} dt, \quad (5c)$$

where T is the averaging time. As we will see, the processes in (3) and (4), although having the same spectra and covariance functions, display considerable differences when it comes to estimating the covariances (5). In particular, we will show that the convergence, as $T \rightarrow \infty$, of the covariance estimates to their respective expectations depend on the structures of $d\mu_x$ and $d\mu_y$, as well as on the choice of model (3) or (4). Specifically, we are interested in under what conditions the estimators in (5) are consistent estimators. A motivating example illustrating these problems is presented in the next section.

III. MOTIVATING EXAMPLES

Consider an array processing scenario in which two sources, emitting the signals x and y respectively, impinge on a set of sensors. Considering two of the sensors, the measured signals, s_1 and s_2 , are given by²

$$\begin{aligned} s_1(t) &= x(t - \tau_x^{(1)}) + y(t - \tau_y^{(1)}) \\ s_2(t) &= x(t - \tau_x^{(2)}) + y(t - \tau_y^{(2)}), \end{aligned}$$

where $\tau_x^{(1)}, \tau_x^{(2)}, \tau_y^{(1)}, \tau_y^{(2)}$ are time delays determined by the distance between the sources and the sensors. Then, in order to localize the signal sources [22] or perform noise reduction [23], one typically considers estimates of the array cross-covariance in order to, e.g., fit parametric models [24]. Clearly, the success of such approaches depends on the convergence of empirical moments to their theoretical counterparts, which is determined by the convergence of \hat{r}_x, \hat{r}_y , and \hat{r}_{xy} to their respective expectations. Note that for these problems a continuous-time model of the signal is required in many cases. This is since in array signal processing, the angle or location of signal sources are continuous variables and it is thus not enough to restrict time delays $\tau_x^{(1)}, \tau_x^{(2)}, \tau_y^{(1)}, \tau_y^{(2)}$, and thereby covariance lags, to a discrete grid. Furthermore, unless the signals are perfectly narrowband, time delays cannot simply be modelled as phase shifts of the signal waveforms.

²For simplicity of the exposition, but without loss of generality for the discussion, we here assume lossless propagation.

¹This implies that the singular parts of x and y are uncorrelated.

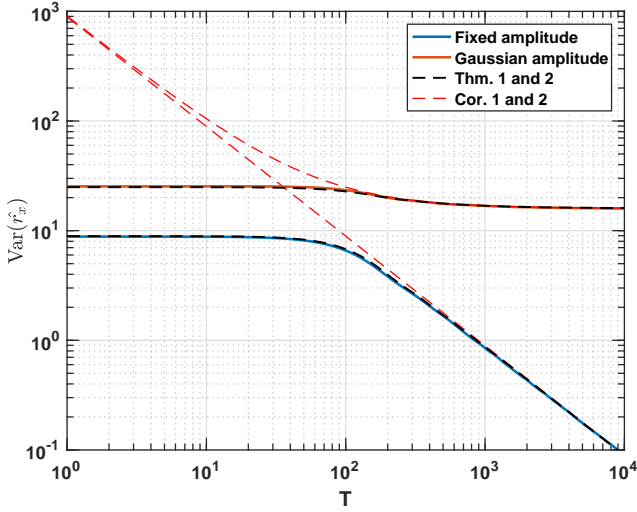


Fig. 1. Empirical variance of auto-covariance estimate as a function of the measurement duration T for a band-limited processes $x = x_a + x_s$, generated according to (4) as well as according to (3). Also presented are finite-sample as well as asymptotic large-sample theoretical values of $\text{Var}(\hat{r}_x(\tau; T))$ according to Theorems 1 and 2, and Corollaries 1 and 2, respectively.

In this setting, consider estimating the auto-covariance, $r_x(\tau)$, of a band-limited stochastic processes $x = x_a + x_s$ realized by the models in (3) or (4), where x_a has a flat spectral density with bandwidth $B = 10^{-2}$, and where x_s consists of a single point mass in located in the same band as the spectrum of x_a . Figure 1 displays the empirical variance, obtained in a Monte Carlo simulation study, of the standard auto-covariance estimate $\hat{r}_x(\tau; T)$ as a function of the averaging time T . As can be seen, for the fixed amplitude model, the variance tends to zero, whereas it for the Gaussian amplitude model converges to a strictly positive number.

Next, introduce a second stochastic process $y = y_s$, independent of x , consisting of two sinusoidal components, and thus the spectrum consists of two point masses. Let the frequencies of the point masses belong to the same band as the spectrum of x_a , and consider two scenarios. Firstly, when both point masses are distinct from the point mass of x_s , and secondly, when one of the point masses of y_s is located at the frequency corresponding to the point mass of x_s . Figure 2 shows the empirical variance of the cross-covariance estimate $\hat{r}_{xy}(\tau; T)$ for these two scenarios. As can be seen, for the first scenario with no common point mass, the estimator variance tends to zero as T increases, whereas for the second scenario with a common point mass, the variance remains bounded away from zero. It may be noted that Figures 1 and 2 in addition to the empirical variances also show theoretically computed finite-sample and asymptotic values of the estimator variance. In the following section, we derive closed-form expressions for these quantities, explaining the observations from the examples.

IV. ESTIMATING THE COVARIANCE FUNCTION

As seen in the previous section, the variance of the cross-covariance estimate, i.e., $\text{Var}(\hat{r}_{xy}(\tau; T))$, behaves dramatically different depending on whether or not the spectra $d\mu_x$ and $d\mu_y$ have common point masses; if singular components are

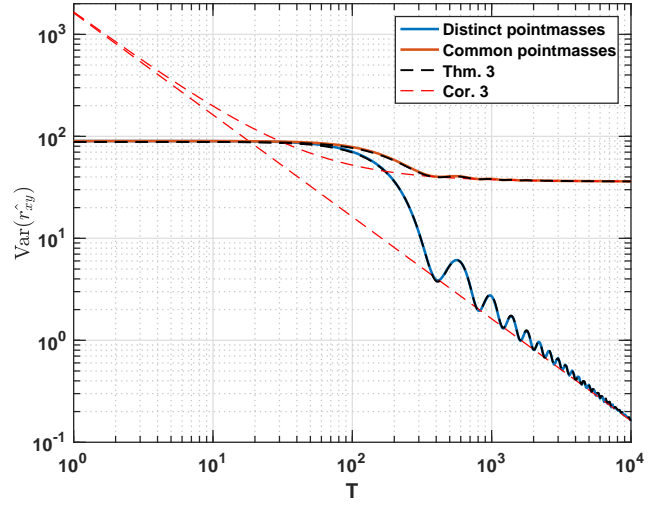


Fig. 2. Empirical variance of cross-covariance estimate as a function of the measurement duration T for two band-limited processes $x = x_a + x_s$ and $y = y_s$, generated according to (4), with both distinct and common point masses. Also presented are finite-sample as well as asymptotic large-sample theoretical values of $\text{Var}(\hat{r}_{xy}(\tau; T))$ according to Theorem 3 and Corollary 3, respectively.

shared, the variance does not tend to zero, i.e., r_{xy} cannot be consistently estimated. Furthermore, the auto-covariance function r_x could only be consistently estimated by $\hat{r}_x(\cdot; T)$ when the singular parts of the spectrum were modeled by fixed-amplitude components as in (4). In order to explain this, we in Theorems 1 and 2 present closed-form expressions for the auto-covariance estimate \hat{r}_x when models (3) and (4) are considered, respectively. Theorem 3 presents the corresponding expression for the finite-sample variance of \hat{r}_{xy} , corresponding to both models (3) and (4). Furthermore, asymptotic expressions, i.e., valid as $T \rightarrow \infty$, for the respective quantities are presented in corresponding corollaries.

In the expressions for the estimator variance in the theorems, the continuous-time counterpart of the Fejér kernel [13],

$$\begin{aligned} f_T(\theta) &\triangleq \int_{t=-T}^T (1 - |t|/T) e^{i2\pi\theta t} dt \\ &= \frac{2}{\theta^2 T (2\pi)^2} (1 - \cos(2\pi\theta T)), \end{aligned} \quad (6)$$

appears naturally. The kernel f_T has several interesting properties that will be used in the derivations of the theorems; in particular, f_T acts as an approximate identity in convolutions. Letting $*$ denote convolution, we summarize these properties in the following proposition.

Proposition 1 (Properties of f_T). *The following properties of f_T hold.*

- For all $T > 0$, $f_T(\theta) \geq 0$ for all $\theta \in \mathbb{R}$.
- For all $T > 0$, $\lim_{\theta \rightarrow 0} f_T(\theta) = T$.
- For all $\theta \neq 0$, $\lim_{T \rightarrow \infty} f_T(\theta) = 0$.
- For all $T > 0$, $\int_{-\infty}^{\infty} f_T(\theta) d\theta = 1$.
- For any $\Phi \in L_1(\mathbb{R})$, $f_T * \Phi \rightarrow \Phi$ in L_1 as $T \rightarrow \infty$.

Proof. The first four properties are easily verified. For the last property, see, e.g., [25, Chapter 2]. \square

With this, we are ready to state the theorems providing the theoretical estimator variances illustrated in Figures 1 and 2.

Theorem 1. *Let x be as in (3). Then, the variance of the auto-covariance estimate is given by*

$$\text{Var}(\hat{r}_x(\tau; T)) = \frac{1}{T} \int_{\theta} \int_{\phi} f_T(\theta - \phi) d\mu_x(\theta) d\mu_x(\phi).$$

Proof. See appendix. \square

Remark 1. *It may be noted that, perhaps surprisingly, the estimator variance does not depend on the lag τ . This is due to the same averaging time, T , is used, irrespective of the lag. This is the relevant case for array processing; the covariance components constituting the array covariance matrix are all estimated from a common data length. All presented results may, in a straightforward manner, be modified as to account for other averaging times and time windows.*

It may be noted that the variance of the estimator is related to the concentration of mass as described by the spectrum $d\mu_x$. The asymptotic variance is thus given in the following corollary.

Corollary 1. *Let x be as in (3) and assume that Φ_x is continuous in the points θ_k^x for $k = 1, \dots, N_x$. Then, as $T \rightarrow \infty$,*

$$T \text{Var}(\hat{r}_x(\tau; T)) - \Psi_T \rightarrow 0,$$

where

$$\Psi_T = \int_{\theta} \Phi_x(\theta)^2 d\theta + 2 \sum_{k=1}^{N_x} \alpha_k^2 \Phi_x(\theta_k^x) + T \sum_{k=1}^{N_x} \alpha_k^4.$$

Proof. The result follows directly by applying Theorem 1 in the same way as Theorem 3 is applied in the proof of Corollary 3. \square

Here, it may be noted that the variance of $\hat{r}_x(\cdot; T)$ does not tend to zero as $T \rightarrow \infty$ when the process contains a sinusoidal component. This is since the statistical moments cannot be estimated from single realizations of the process. This is a consequence of the amplitudes, and in particular the magnitudes, of the sinusoidal components of (3) being stochastic. However, if we consider (4), which is not ergodic either, a different result emerges, as detailed in the following theorem.

Theorem 2. *Let x be as in (4). Then, the variance of the auto-covariance estimate is given by*

$$\text{Var}(\hat{r}_x(\tau; T)) = \frac{1}{T} \int_{\theta} \int_{\phi} f_T(\theta - \phi) d\mu_x(\theta) d\mu_x(\phi) - \sum_{k=1}^{N_x} \alpha_k^4.$$

Proof. See appendix. \square

Here, it may be noted that as compared to Theorem 1, a term corresponding to the amplitudes of the sinusoidal components is subtracted. This term results from the amplitudes of the sinusoids being fixed and only the initial phases being stochastic. As a direct consequence, the variance of $\hat{r}_x(\tau; T)$ is always lower when using the model (4) as compared to (3).

Furthermore, for (4), the auto-covariance can be consistently estimated, as shown in the following corollary.

Corollary 2. *Let x be as in (4) and assume that Φ_x is continuous in the points θ_k^x for $k = 1, \dots, N_x$. Then, as $T \rightarrow \infty$,*

$$T \text{Var}(\hat{r}_x(\tau; T)) - \Psi'_T \rightarrow 0,$$

where

$$\Psi'_T = \int_{\theta} \Phi_x(\theta)^2 d\theta + 2 \sum_{k=1}^{N_x} \alpha_k^2 \Phi_x(\theta_k^x).$$

Proof. The result follows directly by applying Theorem 2 in the same way as Theorem 3 is applied in the proof of Corollary 3. \square

In contrast to the result of Corollary 1, Corollary 2 states that the asymptotic variance $\frac{1}{T} \Psi'_T \rightarrow 0$ as $T \rightarrow \infty$. Furthermore, it may be noted from Theorem 2 for the case of a single sinusoidal component and no component with absolutely continuous spectrum, the estimation error is zero for any positive T . It may here be noted that asymptotic variance expression of Corollary 2 coincides with that of [18, Theorem 2]. However, in the latter, the result holds for mixed-spectrum processes where the component with the density is a (not necessarily Gaussian) moving average process, whereas the result derived herein concerns Gaussian processes with general densities.

The results concerning the estimation of the auto-covariance of a signal can be extended to the case where the cross-covariance is estimated. The following theorem holds.

Theorem 3. *Let x and y be as in (3) or (4). Then, the variance of the cross-covariance estimate is given by*

$$\begin{aligned} \text{Var}(\hat{r}_{xy}(\tau; T)) &= \mathbb{E}(|\hat{r}_{xy}(\tau; T)|^2) - |\mathbb{E}(\hat{r}_{xy}(\tau; T))|^2 \\ &= \frac{1}{T} \int_{\theta} \int_{\phi} f_T(\theta - \phi) d\mu_x(\theta) d\mu_y(\phi). \end{aligned}$$

Proof. See appendix. \square

As can be seen from Theorem 3, $\hat{r}_{xy}(\tau; T)$ is an unbiased estimator of $r_{xy}(\tau)$, with a variance that depends on the overlap of the spectra $d\mu_x$ and $d\mu_y$. However, it is not necessarily a consistent estimator, as shown in Corollary 3.

Corollary 3. *Let x and y be as in (3) or (4) and assume that Φ_y is continuous in the points θ_k^x for $k = 1, \dots, N_x$, and that Φ_x is continuous in the points θ_{ℓ}^y for $\ell = 1, \dots, N_y$. Then, as $T \rightarrow \infty$,*

$$T \text{Var}(\hat{r}_{xy}(\tau; T)) - \Psi''_T \rightarrow 0,$$

where

$$\begin{aligned} \Psi''_T &= \int_{\theta} \Phi_x(\theta) \Phi_y(\theta) d\theta + \sum_{k=1}^{N_x} \alpha_k^2 \Phi_y(\theta_k^x) + \sum_{k=1}^{N_y} \beta_k^2 \Phi_x(\theta_k^y) \\ &\quad + T \sum_{k=1}^{N_x} \sum_{\ell=1}^{N_y} \alpha_k^2 \beta_{\ell}^2 \chi_{\{\theta_k^x = \theta_{\ell}^y\}} \end{aligned}$$

and where χ is the characteristic function.

Proof. See the appendix. \square

It may be noted that if the two signals share sinusoidal components, then Ψ_T'' is not bounded as $T \rightarrow \infty$. Also in general, the asymptotic variance, $\frac{1}{T}\Psi_T''$ tends to

$$\lim_{T \rightarrow \infty} \frac{1}{T}\Psi_T'' = \sum_{k=1}^{N_x} \sum_{\ell=1}^{N_y} \alpha_k^2 \beta_\ell^2 \chi_{\{\theta_k^x = \theta_\ell^y\}},$$

which is strictly positive if any sinusoidal frequencies are common. Interestingly, the issue of ergodicity is only apparent if point masses are shared; if all sinusoidal frequencies are distinct, the estimator variance tends to zero.

The results of Theorems 1, 2, and 3, have implications for inference for array processing applications. In fact, if mixed-spectrum processes are considered and the signals are generated according to (4), then the array covariance function can be consistently estimated as long as the individual processes do not share any sinusoidal components. In contrast, if the model (3) is used, the array covariance cannot be estimated as the estimates of the auto-covariance functions do not converge to their expectations. Furthermore, these results have implications for how to approximate processes with absolutely continuous spectra, as we will see next.

V. APPROXIMATIONS OF CONTINUOUS SPECTRA

Consider the problem of generating realizations from a Gaussian process x with a continuous spectral density $\Phi \in C(\mathcal{I}_B)$ as to, e.g., simulate broadband array signals. To this end, one may³ approximate the target signal using processes with completely singular spectra, i.e., sinusoidal models. Then, one may ask whether to utilize the Gaussian amplitude model in (3) or the fixed amplitude model (4) and, in particular, how such approximations behave in covariance estimation. As formalized in the following theorem, both models allow for approximating a process with a spectral density Φ .

Theorem 4. *Let $x(t)$ be a band-limited Gaussian WSS process with a continuous spectrum $\Phi \in C(\mathcal{I}_B)$ with support in $\mathcal{I}_B = [\theta_c - B/2, \theta_c + B/2]$, where θ_c is the center frequency and B is the bandwidth. Define the sequence of approximating processes*

$$x^{(n)}(t) = \sum_{k=1}^n \sqrt{\frac{B}{n}} \Phi(\theta_k^{(n)}) e^{i2\pi\theta_k^{(n)}t} z_k^{(n)}, \quad (7)$$

where the frequency points $\theta_k^{(n)} = \theta_c + B \frac{k-1-n/2}{n}$ for $k = 1, \dots, n$, define a uniform grid on \mathcal{I}_B . Here $z_k^{(n)}$ are independent identically distributed random variables, either distributed as $z_k^{(n)} \sim \mathcal{CN}(0, 1)$ or $z_k^{(n)} = e^{i\varphi_k^{(n)}}$, where $\varphi_k^{(n)} \sim \mathcal{U}([-\pi, \pi])$. Then, the sequence of processes $\{x^{(n)}\}_n$ converges to x in distribution when $n \rightarrow \infty$.

Proof. See appendix. \square

³Alternatively, one could, e.g., consider sampling from an ARMA process with the correct spectral shape in the band \mathcal{I}_B , together with appropriate bandpass filtering.

Remark 2. *The result of Theorem 4 may be generalized in a straightforward manner to spectral densities Φ that are piecewise continuous with a finite number of discontinuities.*

Thus, constructing approximations from either (3) or (4) yield processes that converge in distribution to any given process x when the number of point masses, n , tends to infinity. To see that this is consistent with Theorems 1 and 2, i.e., that the covariance estimator for such approximation should in the limit behave as for the process x , it may be noted that, as a consequence of Lemma 1,

$$d\mu^{(n)}(\theta) = \sum_{k=1}^n \frac{B}{n} \Phi(\theta_k^{(n)}) \delta(\theta - \theta_k^{(n)}) \xrightarrow{*} \Phi(\theta),$$

where $\xrightarrow{*}$ denotes weak* convergence. Then, as f_T is continuous for any finite T ,

$$\begin{aligned} \int_{\theta} \int_{\phi} f_T(\theta - \phi) d\mu^{(n)}(\theta) d\mu^{(n)}(\phi) \\ \rightarrow \int_{\theta} \int_{\phi} f_T(\theta - \phi) \Phi(\theta) \Phi(\phi) d\theta d\phi, \end{aligned}$$

as $n \rightarrow \infty$. Furthermore, the extra term related to the sinusoidal amplitudes in Theorem 2 is given by

$$\begin{aligned} A(n) &\triangleq \sum_{k=1}^n \left(\frac{B}{n} \Phi(\theta_k^{(n)}) \right)^2 = \frac{1}{n^2} \sum_{k=1}^n \left(B \Phi(\theta_k^{(n)}) \right)^2, \\ &\leq \frac{B^2}{n} \max_{\theta \in \mathcal{I}_B} \Phi(\theta)^2, \end{aligned}$$

and since Φ is bounded,⁴ we have that $A(n) \rightarrow 0$ as $n \rightarrow \infty$. Thus, Theorems 1 and 2 predict the correct limiting behavior of approximations constructed according to Theorem 4. It may however be noted that this is only valid if T is fixed. In order to obtain a description of the behavior of the covariance estimators in the asymptotic regime, i.e., when both n and T are large, we consider the following theorem.

Theorem 5. *Let $x^{(n)}$ be processes with spectrum $d\mu^{(n)}$, approximating the process x with a continuous spectrum Φ , as in Theorem 4, and let $\hat{r}_x^{(n)}(\tau; T)$ be the corresponding covariance estimate as in (5a). Let $n \rightarrow \infty, T \rightarrow \infty$ with $T \frac{B}{n} \rightarrow \gamma$, then*

$$T \text{Var} \left(\hat{r}_x^{(n)}(\tau; T) \right) \rightarrow \rho(\gamma) \int_{\mathcal{I}_B} \Phi(\theta)^2 d\theta$$

for the fixed amplitude model, and

$$T \text{Var} \left(\hat{r}_x^{(n)}(\tau; T) \right) \rightarrow (\gamma + \rho(\gamma)) \int_{\mathcal{I}_B} \Phi(\theta)^2 d\theta$$

for the Gaussian amplitude model, where

$$\rho(\gamma) = \frac{\check{\gamma}(1 - \check{\gamma})}{\gamma}$$

and $\check{\gamma}$ is the decimal part⁵ of γ .

Proof. See the appendix. \square

⁴Note that Φ is continuous on a compact interval.

⁵That is, $\check{\gamma} = \gamma - \lfloor \gamma \rfloor$ where $\lfloor \gamma \rfloor$ denotes the integer part of γ .

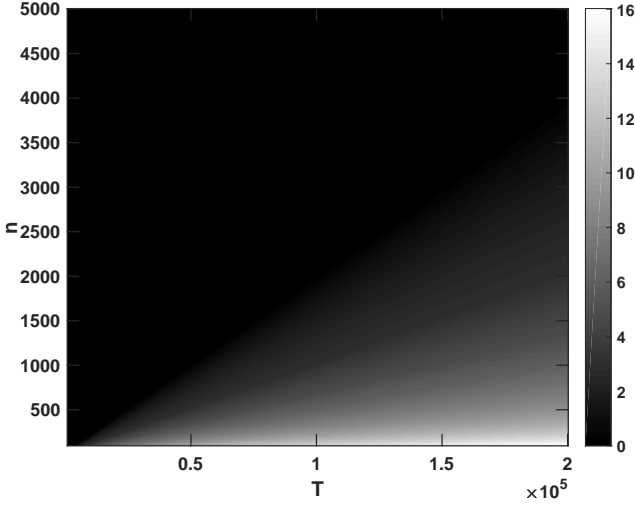


Fig. 3. The asymptotic variance factor $\gamma + \rho(\gamma)$, where $\gamma = T \frac{B}{n}$, for the Gaussian amplitude approximation in Theorem 4, presented as $10 \log_{10}(\gamma + \rho(\gamma))$, for large T and n , as given by Theorem 5. Here, the bandwidth is $B = 2 \times 10^{-2}$.

Remark 3. It may be noted that for $\gamma \in (0, 1]$, $\rho(\gamma) = 1 - \gamma$, and thus $\gamma + \rho(\gamma) \equiv 1$. Thus, for $n \geq BT$, the Gaussian amplitude approximation behaves as the target process, i.e., the asymptotic estimator variance is $\frac{1}{T} \int_{\mathcal{I}_B} \Phi(\theta)^2 d\theta$. For the fixed amplitude approximation to mimic the target process, it is required that $n \gg BT$, as $\lim_{\gamma \rightarrow 0} \rho(\gamma) = 1$. It may be noted that $\rho(\gamma) \in [0, 1)$ for any finite γ , i.e., the variance for the fixed amplitude approximation is always lower than that of the target process. In fact, $\rho(\gamma) = 0$ for $\gamma \in \mathbb{N}$, i.e., the variance is exactly zero for integer γ . Furthermore, it is readily verified that $\gamma + \rho(\gamma)$ is continuous, monotone increasing, and that $\lim_{\gamma \rightarrow \infty} \rho(\gamma) = 0$, implying that the variance of the Gaussian amplitude approximation is larger than that of the target process for all $\gamma > 1$. In particular, for $\gamma > 1$, the asymptotic variance for the Gaussian amplitude approximation is $\frac{B}{n} \int_{\mathcal{I}_B} \Phi(\theta)^2 d\theta > \frac{1}{T} \int_{\mathcal{I}_B} \Phi(\theta)^2 d\theta$.

Remark 4. The proof of Theorem 5 is based on the fact that

$$\sum_{m=-\infty}^{\infty} f_{\gamma}(m) = \gamma + \rho(\gamma),$$

where f_{γ} is the Fejér kernel defined in (6). Therefore, the variance expression connects directly to the sampling of the frequency band used in the approximation.

The parameter γ is the product of the measurement duration T and the frequency resolution B/n of the discretization. According to Theorem 5, the finer the frequency resolution is in relation to the measurement time, the more the singular approximations behave as a process with a spectral density, whereas the properties pertaining from the singular spectra become more apparent when T is large in relation to B/n . For large but finite n , we have that the approximation based on the fixed amplitude model has the property that the finite-sample variance for the covariance estimator is lower than its Gaussian amplitude counterpart. Thus, even though both models in the limit, i.e., as $n \rightarrow \infty$, are identical to the process x , they can for finitely many components behave dramatically different. In

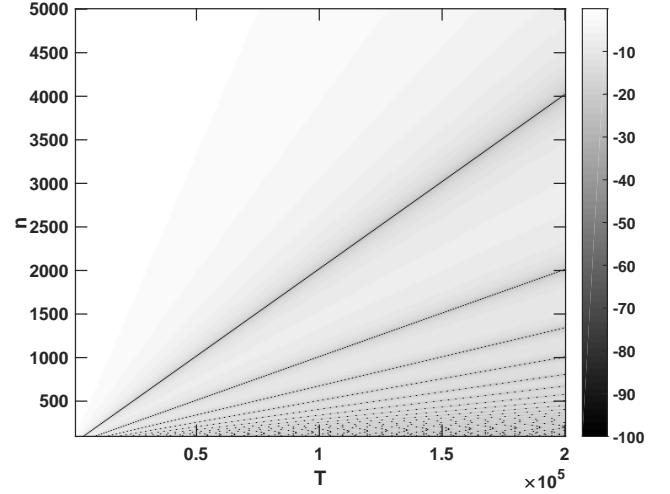


Fig. 4. The asymptotic variance factor $\rho(\gamma)$, where $\gamma = T \frac{B}{n}$, for the fixed amplitude approximation in Theorem 4, presented as $10 \log_{10}(\rho(\gamma))$, for large T and n , as given by Theorem 5. Here, the bandwidth is $B = 2 \times 10^{-2}$.

particular, if using fixed amplitude approximations according to Theorem 4 with finite n as to, e.g., generate test data for array processing, one runs the risk obtaining too well-behaved results as compared to if an actual process x with a spectral density would be used.

VI. NUMERICAL ILLUSTRATIONS

In this section, we illustrate the results of the presented theorems by numerical examples.

A. Asymptotics for singular approximations

To demonstrate the results of Theorem 5, Figures 3 and 4 present the scaling factors $\gamma + \rho(\gamma)$ and $\rho(\gamma)$, corresponding to the Gaussian amplitude and fixed amplitude approximations, respectively, for varying values of n and T . Here, the bandwidth is fixed to $B = 2 \times 10^{-2}$. As can be seen from Figure 3, the scaling factor for the Gaussian amplitude model is bounded from below by 1, which is attained for $\gamma \leq 1$, corresponding to values of n that are large relative to T . In contrast, as can be seen in Figure 4, the scaling factor only asymptotically approaches 1 from below as $\gamma \rightarrow 0$, i.e., as n grows in relation to T . Furthermore, it may be noted that the scaling factor is exactly zero for finite n and T corresponding to integer values of γ .

B. Estimator variance for singular approximations

To illustrate the behavior of the singular approximations of processes with spectral densities, consider the spectrum

$$\Phi(\theta) = \begin{cases} \frac{1}{B} & \theta \in \mathcal{I}_B \\ 0 & \theta \notin \mathcal{I}_B, \end{cases} \quad (8)$$

where the center frequency and bandwidth of \mathcal{I}_B are $\omega_c = 1$ and $B = 10^{-2}$, respectively. We then approximate Φ according to Theorem 4 using both the fixed amplitude model and the model with Gaussian amplitudes. In both cases we, consider approximations with $n = 100$ and $n = 1000$ components.

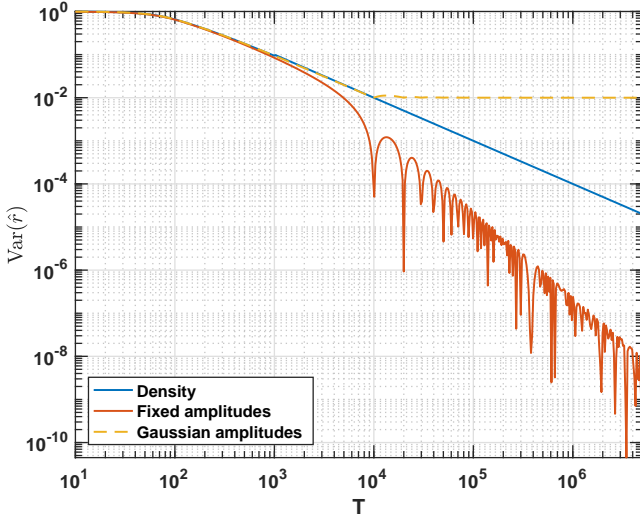


Fig. 5. Variance for the covariance estimator for a covariance function corresponding to an absolutely continuous process, as well as for singular approximations according to Theorem 4 for $n = 100$.

Letting r_a and $r_s^{(n)}$ denote the covariance functions corresponding to Φ and a singular approximation with n components, respectively, where it may be noted that the covariance function for the two singular approximations are identical, let $\epsilon : \mathbb{R} \times \mathbb{N} \rightarrow \mathbb{R}_+$ be defined as

$$\epsilon(\tau, n) \triangleq \sqrt{\frac{\int_0^\tau |r_a(t) - r_s^{(n)}(t)|^2 dt}{\int_0^\tau |r_a(t)|^2 dt}},$$

i.e., the relative L_2 error when considering the covariance up to lag τ . In this case, considering a maximum lag of $\tau = 100$, we have $\epsilon(100, 100) = 1 \times 10^{-6}$ and $\epsilon(100, 1000) = 2 \times 10^{-7}$ for the approximations with $n = 10$ and $n = 100$ components, respectively. With this, Figures 5 and 6 display the variance of the estimators \hat{r}_a and $\hat{r}_s^{(n)}$ as a function of the measurement duration T , for $n = 100$ and $n = 1000$, respectively. The estimator variances are computed according to Theorems 1 and 2. As can be seen, the variance corresponding the fixed amplitude model is consistently lower than that of the process with a density. Furthermore, even though the Gaussian amplitude model mimics the target process perfectly for $T \leq \frac{n}{B}$, the variance does not tend to zero as $T \rightarrow \infty$. In fact, the variance stabilizes for $T \geq 10^4$ and $T \geq 10^5$ for $n = 100$ and $n = 1000$, respectively, corresponding to $\gamma \leq 1$, as predicted by Theorem 5.

C. Implications for array processing: DoA estimation

As noted, the two alternatives for constructing the singular approximations (7) in Theorem 4 differ considerably in terms of their behavior in covariance estimation. To illustrate the implication of this for array processing, we consider a simple DoA estimation example where two sources, both with spectra as in (8), i.e., spectral densities, with bandwidth $B = 10^{-3}$ and center frequency $\theta_c = 0.25$, impinge from angles -5 degrees and 10 degrees, respectively, on a uniform linear array consisting of 10 sensors with inter-sensor spacing just

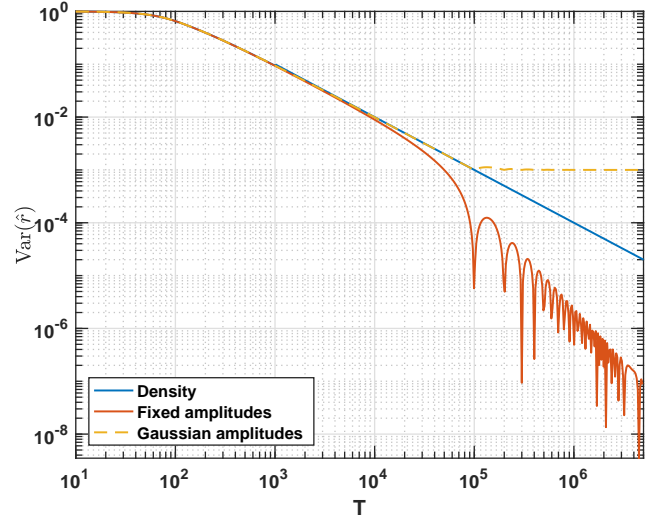


Fig. 6. Variance for the covariance estimator for a covariance function corresponding to an absolutely continuous process, as well as for singular approximations according to Theorem 4 for $n = 1000$.

below half of the highest frequency in the support of (8). We add a spatially and temporally white Gaussian sensor noise to the sensor signals, yielding a signal-to-noise-ratio (SNR) of 10 dB. The array covariance matrix is estimated as the sample covariance matrix, averaging $T = 5 \times 10^5$ consecutive array snapshots. It may here be noted that the snapshots are not independent as consecutive samples are considered. The spatial spectrum is estimated by integrating the narrowband Capon⁶ spatial spectrum [8] over the frequency band \mathcal{I}_B . This is performed for singular approximations of the signals with spectral densities, constructed according to (7) in Theorem 4. For these approximations, we consider varying the parameter γ , and thereby n as T and B are fixed, between $\gamma = 0.5$, corresponding to $n = 1000$, and $\gamma = 5$, corresponding to $n = 100$. As to avoid the problem of non-vanishing variance observed in Corollary 3, the singular components of the second source are shifted in frequency by $B/2n$ as to avoid any overlap. The procedure is repeated in 100 Monte Carlo simulations. The per-angle mean squared error (MSE) for the estimated spatial spectra⁷ are presented in Figures 7 and 8 for the fixed amplitude and Gaussian amplitude approximations, respectively. As reference, the corresponding MSE of the estimated spatial spectrum for the target process with spectral density, generated by bandpass filtering white noise using a Butterworth filter with passband \mathcal{I}_B , is also presented. It may be noted that all values are normalized by the largest per-angle MSE corresponding to the filtered process. As can be seen in Figure 7, the MSE of the spatial spectrum corresponding to the fixed amplitude approximation is lower than that of the filtered process for all considered values of γ . One may here

⁶As the Capon spectral estimator is non-linear in the array covariance matrix estimates, the results from Theorem 5 can only be expected to hold qualitatively.

⁷The reference is the corresponding Capon spectrum computed using the exact array covariance matrix. It may be noted that the approximations incur a bias due to the discretization. However, for the considered values of γ , the squared bias is two orders of magnitude smaller than the variance corresponding to the process with a density.

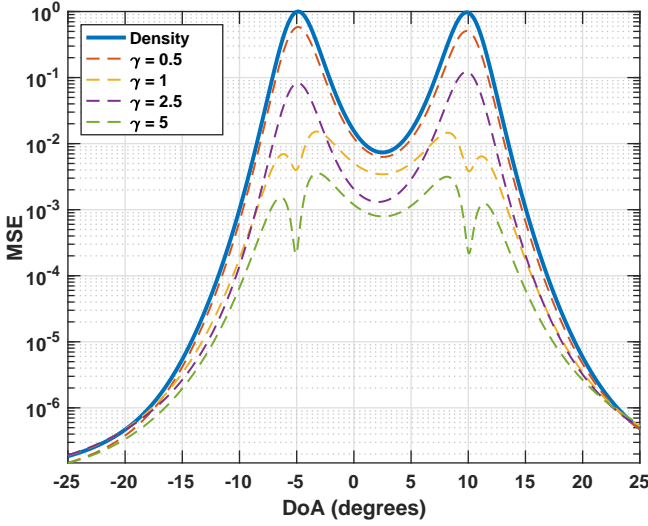


Fig. 7. The MSE of the Capon spatial spectrum, integrated over \mathcal{I}_B , for two signals with spectral densities, both of bandwidth $B = 10^{-3}$, impinging from -5 degrees and 10 degrees, when approximated according to (7) using the fixed amplitude model for a measurement duration of $T = 5 \times 10^5$. The number n of discretization components vary with the parameter γ from Theorem 5.

recall from Theorem 5 that it is required that $\gamma \rightarrow 0$ for the variance of the covariance estimate to converge to that of the process with spectral density. Furthermore, a drop in the MSE may be observed for integer values of γ . For these values, the autocovariances for the two sources are perfectly estimated (c.f. Theorem 5), and the variability stems from the sensor noise and the non-zero variance of the estimates of the sources' cross-covariance. It may here be noted that the MSE does not strictly decrease with increasing γ as ρ is not monotone. In contrast, the MSE for the Gaussian amplitude approximation coincides with that of the filtered process for $\gamma \leq 1$, whereas being higher for $\gamma > 1$, in accordance with Theorem 5.

VII. CONCLUSIONS

In this work, we have derived exact finite-sample as well as asymptotic large-sample expressions for the statistical variance of covariance function estimates for mixed-spectrum signals. As has been shown, the statistical properties of such estimates differ considerably depending on how the singular part of the spectrum is modeled. Furthermore, for singular approximations of processes with continuous spectra, we have presented asymptotic regime results for the covariance estimator variance when both the measurement time and the number of approximating components tend to infinity. As has been illustrated, the difference in variability of the covariance estimates corresponding to the different approximations have a considerable impact on the statistical performance of array processing algorithms.

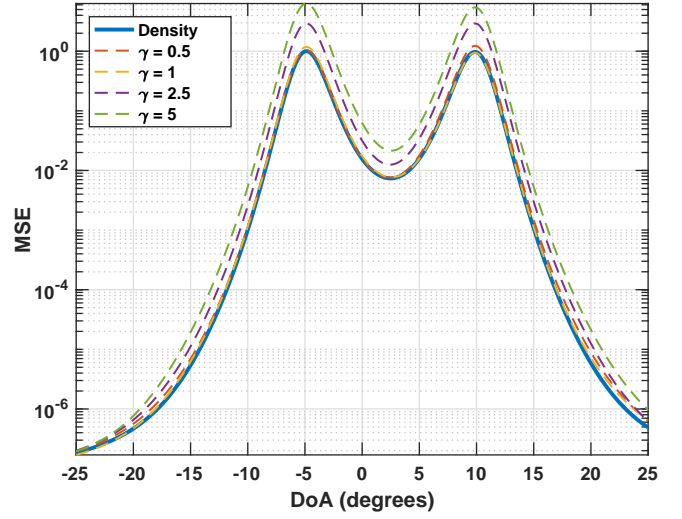


Fig. 8. The MSE of the Capon spatial spectrum, integrated over \mathcal{I}_B , for two signals with spectral densities, both of bandwidth $B = 10^{-3}$, impinging from -5 degrees and 10 degrees, when approximated according to (7) using the Gaussian amplitude model for a measurement duration of $T = 5 \times 10^5$. The number n of discretization components vary with the parameter γ from Theorem 5.

APPENDIX

A. Proof of Theorem 1

Proof. Since x is Gaussian, circularly symmetric, and zero-mean, we have that

$$\begin{aligned} & \mathbb{E} \left(x(t) \overline{x(t-\tau)} \overline{x(\sigma)} x(\sigma-\tau) \right) \\ &= \mathbb{E} \left(x(t) \overline{x(t-\tau)} \right) \mathbb{E} \left(\overline{x(\sigma)} x(\sigma-\tau) \right) \\ & \quad + \mathbb{E} \left(x(t) \overline{x(\sigma)} \right) \mathbb{E} \left(\overline{x(t-\tau)} x(\sigma-\tau) \right) \\ &= r_x(\tau) r_x(-\tau) + r_x(t-\sigma) r_x(\sigma-t) \\ &= |r_x(\tau)|^2 + |r_x(t-\sigma)|^2. \end{aligned}$$

Using this, it can be noted that

$$\begin{aligned} & \mathbb{E} \left(|\hat{r}_x(\tau; T)|^2 \right) \\ &= \mathbb{E} \left[\left(\frac{1}{T} \int_{t=0}^T x(t) \overline{x(t-\tau)} dt \right) \left(\frac{1}{T} \int_{s=0}^T \overline{x(\sigma)} x(\sigma-\tau) d\sigma \right) \right] \\ &= \frac{1}{T^2} \int_{t=0}^T \int_{\sigma=0}^T \mathbb{E} \left(x(t) \overline{x(\sigma)} \right) \mathbb{E} \left(x(\sigma-\tau) \overline{x(t-\tau)} \right) dt d\sigma \\ & \quad + \frac{1}{T^2} \int_{t=0}^T \int_{\sigma=0}^T \mathbb{E} \left(x(t) \overline{x(t-\tau)} \right) \mathbb{E} \left(x(\sigma-\tau) \overline{x(\sigma)} \right) dt d\sigma \\ &= \frac{1}{T^2} \int_{t=0}^T \int_{\sigma=0}^T (r_x(t-\sigma) r_x(\sigma-t) + r_x(\tau) r_x(\tau)) dt d\sigma \\ &= \frac{1}{T^2} \int_{t=0}^T \int_{\sigma=0}^T r_x(t-\sigma) r_x(\sigma-t) dt d\sigma + |r_x(\tau)|^2. \end{aligned}$$

Next, since $\mathbb{E}(\hat{r}_x(\tau; T)) = r_x(\tau)$, the variance is

$$\begin{aligned} \text{Var}(\hat{r}_x(\tau; T)) &= \mathbb{E}(|\hat{r}_x(\tau; T)|^2) - |\mathbb{E}(\hat{r}_x(\tau; T))|^2 \\ &= \mathbb{E}(|\hat{r}_x(\tau; T)|^2) - |r_x(\tau)|^2 \\ &= \frac{1}{T^2} \int_{t=0}^T \int_{\sigma=0}^T r_x(t-\sigma) r_x(\sigma-t) dt d\sigma \\ &= \frac{1}{T^2} \int_{t=0}^T \int_{\sigma=0}^T \int_{\theta} e^{i2\pi\theta(t-\sigma)} d\mu_x(\theta) \int_{\phi} e^{i2\pi\phi(\sigma-t)} d\mu_x(\phi) dt d\sigma \\ &= \frac{1}{T^2} \int_{\theta} \int_{\phi} \left(\int_{t=0}^T \int_{\sigma=0}^T e^{i2\pi(\theta-\phi)(t-\sigma)} dt d\sigma \right) d\mu_x(\theta) d\mu_x(\phi) \\ &= \frac{1}{T} \int_{\theta} \int_{\phi} \left(\int_{t=-T}^T (1-|t|/T) e^{i2\pi(\theta-\phi)t} dt \right) d\mu_x(\theta) d\mu_x(\phi) \\ &= \frac{1}{T} \int_{\theta} \int_{\phi} f_T(\theta-\phi) d\mu_x(\theta) d\mu_x(\phi). \end{aligned}$$

B. Proof of Theorem 2

Proof. As to simplify notation, let $x(t) = x_a(t) + x_s(t)$, where x_s denotes the sinusoidal part of x . Furthermore, let r_a and r_s be the covariance functions of x_a and x_s , respectively. Then, $\mathbb{E}(\hat{r}_x(\tau; T)) = r_x(\tau) = r_a(\tau) + r_s(\tau)$. Furthermore,

$$\begin{aligned} &\mathbb{E}(|\hat{r}_x(\tau; T)|^2) \\ &= \mathbb{E} \left[\left(\frac{1}{T} \int_{t=0}^T x(t) \overline{x(t-\tau)} dt \right) \left(\frac{1}{T} \int_{t=0}^T \overline{x(t)} x(t-\tau) dt \right) \right] \\ &= \frac{1}{T^2} \int_{t=0}^T \int_{\sigma=0}^T \mathbb{E} \left(x(t) \overline{x(\sigma)} x(\sigma-\tau) \overline{x(t-\tau)} \right) dt d\sigma. \end{aligned}$$

As x_a and x_s are independent, expanding the product yields

$$\begin{aligned} &\mathbb{E} \left(x(t) \overline{x(t-\tau)} \overline{x(\sigma)} x(\sigma-\tau) \right) \\ &= \mathbb{E} \left(x_a(t) \overline{x_a(t-\tau)} \overline{x_a(\sigma)} x_a(\sigma-\tau) \right) \\ &\quad + \mathbb{E} \left(x_s(t) \overline{x_s(t-\tau)} \overline{x_s(\sigma)} x_s(\sigma-\tau) \right) \\ &\quad + \mathbb{E} \left(x_a(t) \overline{x_a(t-\tau)} \right) \mathbb{E} \left(\overline{x_s(\sigma)} x_s(\sigma-\tau) \right) \\ &\quad + \mathbb{E} \left(x_s(t) \overline{x_s(t-\tau)} \right) \mathbb{E} \left(\overline{x_a(\sigma)} x_a(\sigma-\tau) \right) \\ &\quad + \mathbb{E} \left(x_a(t) \overline{x_a(\sigma)} \right) \mathbb{E} \left(\overline{x_s(t-\tau)} x_s(\sigma-\tau) \right) \\ &\quad + \mathbb{E} \left(x_s(t) \overline{x_s(\sigma)} \right) \mathbb{E} \left(\overline{x_a(t-\tau)} x_a(\sigma-\tau) \right) \\ &= \mathbb{E} \left(x_a(t) \overline{x_a(t-\tau)} \overline{x_a(\sigma)} x_a(\sigma-\tau) \right) \\ &\quad + \mathbb{E} \left(x_s(t) \overline{x_s(t-\tau)} \overline{x_s(\sigma)} x_s(\sigma-\tau) \right) \\ &\quad + r_a(\tau) r_s(-\tau) + r_s(\tau) r_a(-\tau) \\ &\quad + r_a(t-\sigma) r_s(\sigma-t) + r_s(t-\sigma) r_a(\sigma-t) \\ &= \mathbb{E} \left(x_a(t) \overline{x_a(t-\tau)} \overline{x_a(\sigma)} x_a(\sigma-\tau) \right) \\ &\quad + \mathbb{E} \left(x_s(t) \overline{x_s(t-\tau)} \overline{x_s(\sigma)} x_s(\sigma-\tau) \right) \\ &\quad + |r_a(t-\sigma) + r_s(t-\sigma)|^2 + |r_a(\tau) + r_s(\tau)|^2 \\ &\quad - |r_a(t-\sigma)|^2 - |r_s(t-\sigma)|^2 - |r_a(\tau)|^2 - |r_s(\tau)|^2. \end{aligned}$$

Furthermore, as x_a is Gaussian, circularly symmetric, and zero-mean,

$$\begin{aligned} &\mathbb{E} \left(x_a(t) \overline{x_a(t-\tau)} \overline{x_a(\sigma)} x_a(\sigma-\tau) \right) \\ &= \mathbb{E} \left(x_a(t) \overline{x_a(t-\tau)} \right) \mathbb{E} \left(\overline{x_a(\sigma)} x_a(\sigma-\tau) \right) \\ &\quad + \mathbb{E} \left(x_a(t) \overline{x_a(\sigma)} \right) \mathbb{E} \left(\overline{x_a(t-\tau)} x_a(\sigma-\tau) \right) \\ &= r_a(\tau) r_a(-\tau) + r_a(t-\sigma) r_a(\sigma-t) \\ &= |r_a(\tau)|^2 + |r_a(t-\sigma)|^2. \end{aligned}$$

Thus,

$$\begin{aligned} &\mathbb{E} \left(x(t) \overline{x(t-\tau)} \overline{x(\sigma)} x(\sigma-\tau) \right) \\ &= \mathbb{E} \left(x_s(t) \overline{x_s(t-\tau)} \overline{x_s(\sigma)} x_s(\sigma-\tau) \right) \\ &\quad + |r_x(t-\sigma)|^2 + |r_x(\tau)|^2 - |r_s(t-\sigma)|^2 - |r_s(\tau)|^2. \end{aligned} \quad (9)$$

To compute the fourth moment of x_s , consider four time points t_1, t_2, t_3 , and t_4 . Then,

$$x_s(t_1) x_s(t_2) \overline{x_s(t_3)} \overline{x_s(t_4)} = \sum_{k, \ell, m, n} \alpha_k \alpha_{\ell} \alpha_m \alpha_n e^{i\xi_{k, \ell, m, n}} \quad (10)$$

where

$$\xi_{k, \ell, m, n} = 2\pi(\theta_k t_1 + \theta_{\ell} t_2 - \theta_m t_3 - \theta_n t_4) + \varphi_k + \varphi_{\ell} - \varphi_m - \varphi_n,$$

and where the superscript of $\varphi_k^{(x)}$ has been suppressed for notational brevity. Since all phases are independent and distributed as $\mathcal{U}((-\pi, \pi])$, the expectation of (10) is only non-zero when $k = m$ and $\ell = n$, or $k = n$ and $\ell = m$. Thus,

$$\begin{aligned} &\mathbb{E} \left(x_s(t_1) x_s(t_2) \overline{x_s(t_3)} \overline{x_s(t_4)} \right) \\ &= \sum_k \sum_{\ell} \alpha_k^2 \alpha_{\ell}^2 \left(e^{i2\pi\theta_k(t_1-t_4) + i2\pi\theta_{\ell}(t_2-t_3)} \right. \\ &\quad \left. + e^{i2\pi\theta_k(t_1-t_3) + i2\pi\theta_{\ell}(t_2-t_4)} \right) - \sum_k \alpha_k^4 e^{i2\pi\theta_k(t_1+t_2-t_3-t_4)}. \end{aligned}$$

Plugging in the corresponding time lags $t_1 = t$, $t_2 = \sigma - \tau$, $t_3 = t - \tau$, and $t_4 = \sigma$, the double sum becomes

$$\begin{aligned} &\sum_k \sum_{\ell} \alpha_k^2 \alpha_{\ell}^2 \left(e^{i2\pi\theta_k(t-\sigma) + i2\pi\theta_{\ell}(\sigma-t)} + e^{i2\pi\theta_k(\tau) + i2\pi\theta_{\ell}(-\tau)} \right) \\ &= \sum_k \alpha_k^2 e^{i2\pi\theta_k(t-\sigma)} \sum_{\ell} \alpha_{\ell}^2 e^{i2\pi\theta_{\ell}(\sigma-t)} \\ &\quad + \sum_k \alpha_k^2 e^{i2\pi\theta_k\tau} \sum_{\ell} \alpha_{\ell}^2 e^{-i2\pi\theta_{\ell}\tau} \\ &= |r_s(t-\sigma)|^2 + |r_s(\tau)|^2. \end{aligned}$$

Noting that $t_1 + t_2 + t_3 + t_4 = 0$, we get

$$\begin{aligned} &\mathbb{E} \left(x_s(t) \overline{x_s(t-\tau)} \overline{x_s(\sigma)} x_s(\sigma-\tau) \right) \\ &= |r_s(t-\sigma)|^2 + |r_s(\tau)|^2 - \sum_k \alpha_k^4. \end{aligned}$$

Inserting this expression in (9) yields

$$\begin{aligned} &\mathbb{E} \left(x(t) \overline{x(t-\tau)} \overline{x(\sigma)} x(\sigma-\tau) \right) \\ &= |r_x(t-\sigma)|^2 + |r_x(\tau)|^2 - \sum_k \alpha_k^4, \end{aligned}$$

and the statement of the theorem follows from the proof of Theorem 1. \square

C. Proof of Theorem 3

Proof. First note that

$$\begin{aligned}
& \mathbb{E} \left(|\hat{r}_{xy}(\tau; T)|^2 \right) \\
&= \mathbb{E} \left[\left(\frac{1}{T} \int_{t=0}^T x(t) \overline{y(t-\tau)} dt \right) \left(\frac{1}{T} \int_{\sigma=0}^T \overline{x(\sigma)} y(\sigma-\tau) d\sigma \right) \right] \\
&= \frac{1}{T^2} \int_{t=0}^T \int_{\sigma=0}^T \mathbb{E} \left(x(t) \overline{x(\sigma)} \right) \mathbb{E} \left(y(\sigma-\tau) \overline{y(t-\tau)} \right) dt d\sigma \\
&+ \frac{1}{T^2} \int_{t=0}^T \int_{\sigma=0}^T \mathbb{E} \left(x(t) \overline{y(t-\tau)} \right) \mathbb{E} \left(y(\sigma-\tau) \overline{x(\sigma)} \right) dt d\sigma \\
&= \frac{1}{T^2} \int_{t=0}^T \int_{\sigma=0}^T (r_x(t-\sigma) r_y(\sigma-t) + r_{xy}(\tau) r_{yx}(\tau)) dt d\sigma \\
&= \frac{1}{T^2} \int_{t=0}^T \int_{\sigma=0}^T r_x(t-\sigma) r_y(\sigma-t) dt d\sigma + |r_{xy}(\tau)|^2.
\end{aligned}$$

Next, since $\mathbb{E}(\hat{r}_{xy}(\tau; T)) = r_{xy}(\tau)$, the variance is

$$\begin{aligned}
& \text{Var}(\hat{r}_{xy}(\tau; T)) = \mathbb{E} \left(|\hat{r}_{xy}(\tau; T)|^2 \right) - |\mathbb{E}(\hat{r}_{xy}(\tau; T))|^2 \\
&= \mathbb{E} \left(|\hat{r}_{xy}(\tau; T)|^2 \right) - |r_{xy}(\tau)|^2 \\
&= \frac{1}{T^2} \int_{t=0}^T \int_{\sigma=0}^T r_x(t-\sigma) r_y(\sigma-t) dt d\sigma \\
&= \frac{1}{T^2} \int_{t=0}^T \int_{\sigma=0}^T \int_{\theta} e^{i2\pi\theta(t-\sigma)} d\mu_x(\theta) \int_{\phi} e^{i2\pi\phi(\sigma-t)} d\mu_y(\phi) dt d\sigma \\
&= \frac{1}{T^2} \int_{\theta} \int_{\phi} \left(\int_{t=0}^T \int_{\sigma=0}^T e^{i2\pi(\theta-\phi)(t-\sigma)} dt d\sigma \right) d\mu_x(\theta) d\mu_y(\phi) \\
&= \frac{1}{T} \int_{\theta} \int_{\phi} \left(\int_{t=-T}^T (1-|t|/T) e^{i2\pi(\theta-\phi)t} dt \right) d\mu_x(\theta) d\mu_y(\phi) \\
&= \frac{1}{T} \int_{\theta} \int_{\phi} f_T(\theta-\phi) d\mu_x(\theta) d\mu_y(\phi).
\end{aligned}$$

D. Proof of Corollary 3

Proof. We have that

$$\begin{aligned}
& \int_{\theta} \int_{\phi} f_T(\theta-\phi) d\mu_x(\theta) d\mu_y(\phi) \\
&= \int_{\theta} \int_{\phi} f_T(\theta-\phi) \Phi_x(\theta) \Phi_y(\phi) d\theta d\phi \\
&+ \sum_k \alpha_k^2 \int_{\theta} \int_{\phi} f_T(\theta-\phi) \delta_{\theta_k^x}(\theta) \Phi_y(\phi) d\theta d\phi \\
&+ \sum_{\ell} \beta_{\ell}^2 \int_{\theta} \int_{\phi} f_T(\theta-\phi) \delta_{\theta_{\ell}^y}(\phi) \Phi_x(\theta) d\theta d\phi \\
&+ \sum_{k,\ell} \alpha_k^2 \beta_{\ell}^2 \int_{\theta} \int_{\phi} f_T(\theta-\phi) \delta_{\theta_k^x}(\theta) \delta_{\theta_{\ell}^y}(\phi) d\theta d\phi.
\end{aligned}$$

First, note that as $\Phi_x, \Phi_y \in L_1$ and as f_T is an approximate identity, it follows that $f_T * \Phi_x \rightarrow \Phi_x$ and $f_T * \Phi_y \rightarrow \Phi_y$ in L_1 , as $T \rightarrow \infty$. Thus,

$$\left| \int_{\theta} \int_{\phi} f_T(\theta-\phi) \Phi_x(\theta) \Phi_y(\phi) d\theta d\phi - \int_{\theta} \Phi_x(\theta) \Phi_y(\theta) d\theta \right| \rightarrow 0$$

and as $\int_{\theta} f_T(\theta-\phi) \delta_{\theta_k^x}(\theta) d\theta = f_T(\theta_k^x - \phi)$,

$$\left| \int_{\theta} \int_{\phi} f_T(\theta-\phi) \delta_{\theta_k^x}(\theta) \Phi_y(\phi) d\theta d\phi - \Phi_y(\theta_k^x) \right| \rightarrow 0$$

as $T \rightarrow \infty$. Finally, $\int_{\theta} \int_{\phi} f_T(\theta-\phi) \delta_{\theta_k^x}(\theta) \delta_{\theta_{\ell}^y}(\phi) d\theta d\phi = f_T(\theta_k^x - \theta_{\ell}^y)$ and

$$|f_T(\theta) - T \chi_{\{\theta=0\}}| \rightarrow 0$$

pointwise as $T \rightarrow \infty$. The statement of the proposition follows directly. \square

E. Proof of Theorem 4

Proof. For both cases $z_k^{(n)} \sim \mathcal{CN}(0, 1)$ and $z_k^{(n)} = e^{i\varphi_k^{(n)}}$, where $\varphi_k^{(n)} \sim \mathcal{U}([-\pi, \pi])$, it by Lemma 1 holds that the covariance function on $x^{(n)}$ converges to the covariance function of x . Thus, for the case $z_k^{(n)} \sim \mathcal{CN}(0, 1)$, the statement of the theorem follows directly as the approximation is Gaussian for any n . For the case $z_k^{(n)} = e^{i\varphi_k^{(n)}}$, we have to show that $x^{(n)}$ converges in distribution to a Gaussian process. Let $\tau \in \mathbb{R}^N$, for $N \in \mathbb{N}$, be a set of sampling times, and let X_k be the random vector defined as $X_k^{(n)} = \begin{bmatrix} x_k^{(n)}(\tau_1) & \dots & x_k^{(n)}(\tau_N) \end{bmatrix}^T$, where $x_k^{(n)}(t) = \sqrt{\frac{B}{n}} \Phi(\theta_k^{(n)}) e^{i2\pi\theta_k^{(n)}t + i\varphi_k^{(n)}}$. Furthermore, let $S_n = \sum_{k=1}^n X_k^{(n)}$. Then, as the vectors $X_k^{(n)}$ are independent, the covariance matrix of S_n is given by

$$\mathbb{E}(S_n S_n^H) = \frac{B}{n} C_n, \quad C_n = \sum_{k=1}^n \Phi(\theta_k^{(n)}) a(\theta_k^{(n)}) a(\theta_k^{(n)})^H,$$

where $a : [-\pi, \pi] \rightarrow \mathbb{C}^N$ is the sub-sampled Fourier vector corresponding to the sampling times τ . Then,

$$\mathbb{E}(S_n S_n^H)^{-1/2} X_k^{(n)} = \sqrt{\Phi(\theta_k^{(n)})} e^{i\varphi_k^{(n)}} C_n^{-1/2} a(\theta_k^{(n)})$$

\square

and

$$\left\| \mathbb{E}(S_n S_n^H)^{-1/2} X_k^{(n)} \right\|_2^2 = \Phi(\theta_k^{(n)}) a(\theta_k^{(n)}) C_n^{-1} a(\theta_k^{(n)}).$$

As Φ is of bounded variation, and as a is a continuous function defined on a compact set, for $n > M$ for some finite M ,

$$C_{2n} \approx 2C_n.$$

Thus, for large n ,

$$a(\theta_k^{(n)}) C_n^{-1} a(\theta_k^{(n)}) \leq c/n$$

where c is a constant not depending on n or k . Then,

$$\begin{aligned}
\sum_{k=1}^n \left\| \mathbb{E}(S_n S_n^H)^{-1/2} X_k^{(n)} \right\|_2^3 &\leq \sum_{k=1}^n \Phi(\theta_k^{(n)})^{3/2} (c/n)^{3/2} \\
&\leq \frac{c^{3/2}}{\sqrt{n}} \sup_{\theta} \Phi(\theta)^{3/2} \rightarrow 0,
\end{aligned}$$

when $n \rightarrow \infty$. According to the Lyapunov-type central limit theorem [26], [27], S_n then converges in distribution to a Gaussian distribution as $n \rightarrow \infty$. This holds for any finite sample length N , with the requirement $N < n$ for invertibility of C_n . The statement of the theorem then follows directly. \square

Lemma 1. Let Φ be a continuous spectrum $\Phi \in C(\mathcal{I}_B)$ with support $\mathcal{I}_B = [\theta_c - B/2, \theta_c + B/2]$, where θ_c is the center frequency and B is the bandwidth. Consider the sequence of stochastic processes

$$x^{(n)}(t) = \sum_{k=1}^n \sqrt{\frac{B}{n}} \Phi(\theta_k^{(n)}) e^{i2\pi\theta_k^{(n)}t} z_k^{(n)},$$

where $\theta_k^{(n)}$ defines a uniform grid on \mathcal{I}_B , and where $z_k^{(n)}$ are independent zero-mean stochastic variables such that $\mathbb{E}(z_k^{(n)} z_k^{(n)}) = 1$. Then, as $n \rightarrow \infty$, the covariance function of $x^{(n)}$ converges to the covariance function defined by Φ as $n \rightarrow \infty$.

Proof. We have

$$\mathbb{E}(x^{(n)}(t) \overline{x^{(n)}(t - \tau)}) = \sum_{k=1}^n \frac{B}{n} \Phi(\theta_k^{(n)}) e^{i2\pi\theta_k^{(n)}\tau}.$$

Then, as Φ continuous on a compact interval, the Riemann sum on the right hand side converges point wise, i.e., for every τ

$$\sum_{k=1}^n \frac{B}{n} \Phi(\theta_k^{(n)}) e^{i2\pi\theta_k^{(n)}\tau} \rightarrow \int_{\mathcal{I}_B} \Phi(\theta) e^{i2\pi\theta\tau} d\theta,$$

which is the covariance function associated with Φ . \square

F. Proof of Theorem 5

Proof. For the approximations in Theorem 4, the approximating spectra are of the form

$$\begin{aligned} d\mu^{(n)}(\theta) &= \sum_{k=1}^n \frac{B}{n} \check{\Phi}\left(\frac{Bk}{n}\right) \delta\left(\theta - \frac{Bk}{n}\right) \\ &= \sum_{k=1}^n \frac{B}{n} \check{\Phi}(\omega) \delta\left(\theta - \frac{Bk}{n}\right) \end{aligned}$$

where, for notational convenience, $\check{\Phi}(\theta) \triangleq \Phi(\theta + \theta_c - B/2)$. Then,

$$\begin{aligned} \int_{\phi} f_T(\theta - \phi) d\mu^{(n)}(\phi) &= \int_{\phi} f_T(\phi) d\mu^{(n)}(\theta - \phi) \\ &= \frac{B}{n} \sum_{m=-\infty}^{\infty} f_T\left(\frac{Bm}{n}\right) \check{\Phi}\left(\theta - \frac{Bm}{n}\right) \\ &= \int_{\phi} \sum_{m=-\infty}^{\infty} \frac{B}{n} f_T(\phi) \delta\left(\phi - \frac{Bm}{n}\right) \check{\Phi}(\theta - \phi) d\phi \\ &= \int_{\phi} f_T^{(n)}(\phi) \check{\Phi}(\theta - \phi) d\phi, \end{aligned}$$

where the summation limits in the second equality follows as the support of Φ is limited to \mathcal{I}_B , and where

$$f_T^{(n)}(\phi) \triangleq \sum_{m=-\infty}^{\infty} f_T(\phi) \delta\left(\phi - \frac{Bm}{n}\right) \frac{B}{n}.$$

According to Lemma 2, $\frac{1}{\gamma + \rho(\gamma)} f_T^{(n)}$ acts as an approximate identity as $n \rightarrow \infty$. Thus, for fixed γ ,

$$\int_{\phi} f_T(\theta - \phi) d\mu^{(n)}(\phi) \rightarrow (\gamma + \rho(\gamma)) \check{\Phi}(\theta).$$

Then, as

$$\int_{\theta} \check{\Phi}(\theta) d\mu^{(n)}(\theta) = \frac{B}{n} \sum_{k=1}^n \left(\check{\Phi}\left(\frac{Bk}{n}\right) \right)^2 \rightarrow \int_{\theta} \check{\Phi}(\theta)^2 d\theta,$$

we have

$$\iint f_T(\theta - \phi) d\mu^{(n)}(\phi) d\mu^{(n)}(\theta) \rightarrow (\gamma + \rho(\gamma)) \int_{\mathcal{I}_B} \Phi(\theta)^2 d\theta.$$

The statement of the theorem then follows directly from Theorems 1 and 2. \square

Lemma 2. Let $\gamma = \frac{BT}{n}$ be fixed. Then, the function

$$\frac{1}{h(\gamma)} f_T^{(n)}(\phi) = \frac{1}{\gamma + \rho(\gamma)} \sum_{m=-\infty}^{\infty} f_T(\phi) \delta\left(\phi - \frac{Bm}{n}\right) \frac{B}{n},$$

parametrized by n , is an approximate identity, i.e., for any $\Phi \in L_1$, $\frac{1}{\gamma + \rho(\gamma)} f_T^{(n)} * \Phi \rightarrow \Phi$ in L_1 as $n \rightarrow \infty$.

Proof. Firstly, note that for any $T > 0$, $f_T(\theta) = T f_1(T\theta)$. We have

$$\begin{aligned} \sum_{m=-\infty}^{\infty} f_T(\phi) \delta\left(\phi - \frac{Bm}{n}\right) \frac{B}{n} &= \sum_{m=-\infty}^{\infty} f_{\frac{BT}{n}}\left(\frac{n}{B}\phi\right) \delta\left(\phi - \frac{Bm}{n}\right) \\ &= \sum_{m=-\infty}^{\infty} f_{\gamma}\left(\frac{n}{B}\phi\right) \delta\left(\phi - \frac{Bm}{n}\right). \end{aligned}$$

Then,

$$\begin{aligned} \int_{-\infty}^{\infty} f_T^{(n)}(\phi) d\phi &= \sum_{m=-\infty}^{\infty} f_{\gamma}(m) = f_{\gamma}(0) + 2 \sum_{m=1}^{\infty} f_{\gamma}(m) \\ &= \gamma + \frac{4}{\gamma(2\pi)^2} \sum_{m=1}^{\infty} \frac{1 - \cos(2\pi\gamma m)}{m^2}. \end{aligned}$$

Clearly, for $\gamma \in \mathbb{N}$, all terms in the series are zero. For non-integer γ , let $\check{\gamma} = \gamma - \lfloor \gamma \rfloor$, with $\lfloor \gamma \rfloor$ denoting the integer part of γ . Then,

$$\begin{aligned} \int_{-\infty}^{\infty} f_T^{(n)}(\phi) d\phi &= \gamma + \frac{1}{\gamma\pi^2} \left(\frac{\pi^2}{6} - \frac{1}{2} (\text{Li}_2(e^{2i\pi\gamma}) + \text{Li}_2(e^{-2i\pi\gamma})) \right) \\ &= \gamma + \frac{1}{\gamma\pi^2} \left(\frac{\pi^2}{6} - \frac{1}{2} (\text{Li}_2(e^{2i\pi\check{\gamma}}) + \text{Li}_2(e^{-2i\pi\check{\gamma}})) \right) \\ &= \gamma + \frac{1}{\gamma\pi^2} \left(\frac{\pi^2}{6} - \frac{1}{2} \left(-\frac{(2i\pi)^2}{2!} B_2(\check{\gamma}) \right) \right) \\ &= \gamma + \frac{\check{\gamma} - \check{\gamma}^2}{\gamma} = \gamma + \rho(\gamma), \end{aligned}$$

where Li_2 is the polylogarithm and B_2 is the Bernoulli polynomial $B_2(x) = x^2 - x + \frac{1}{6}$. Furthermore, letting $n \rightarrow \infty$, and thereby also $T \rightarrow \infty$ as γ is fixed, $f_{\gamma}(\frac{n}{B}\phi) = \frac{B}{n} f_T(\phi) \rightarrow 0$ for $|\phi| > 0$, implying

$$\int_{\phi \notin [-\epsilon, \epsilon]} f_T^{(n)}(\phi) d\phi \rightarrow 0$$

for any $\epsilon > 0$. The statement of the lemma follows. \square

REFERENCES

- [1] H. Krim and M. Viberg, "Two Decades of Array Signal Processing Research," *IEEE Signal Process. Mag.*, pp. 67–94, July 1996.
- [2] H. L. Van Trees, *Detection, Estimation, and Modulation Theory, Part IV, Optimum Array Processing*, John Wiley and Sons, Inc., 2002.
- [3] S. Gannot, E. Vincent, S. Markovich-Golan, and A. Ozerov, "A Consolidated Perspective on Multimicrophone Speech Enhancement and Source Separation," *IEEE/ACM Trans. Audio Speech Lang. Process.*, vol. 25, no. 4, pp. 692–730, 2017.
- [4] M. Trinh-Hoang, M. Viberg, and M. Pesavento, "Cramér-Rao Bound for DOA Estimators Under the Partial Relaxation Framework: Derivation and Comparison," *IEEE Trans. Signal Process.*, vol. 68, pp. 3194–3208, 2020.
- [5] F. Elvander, A. Jakobsson, and J. Karlsson, "Interpolation and Extrapolation of Toeplitz Matrices via Optimal Mass Transport," *IEEE Trans. Signal. Process.*, vol. 66, no. 20, pp. 5285 – 5298, Oct. 2018.
- [6] F. Elvander, I. Haasler, A. Jakobsson, and J. Karlsson, "Multi-marginal optimal transport using partial information with applications in robust localization and sensor fusion," *Signal Process.*, vol. 171, June 2020, Art. no. 107474.
- [7] R. Ali, T. van Waterschoot, and M. Moonen, "Integration of a Priori and Estimated Constraints Into an MVDR Beamformer for Speech Enhancement," *IEEE/ACM Trans. Audio Speech Lang. Process.*, vol. 27, no. 12, pp. 2288–2300, 2019.
- [8] J. Capon, "High Resolution Frequency Wave Number Spectrum Analysis," *Proc. IEEE*, vol. 57, pp. 1408–1418, 1969.
- [9] A. Paulraj, R. Roy, and T. Kailath, "Estimation of Signal Parameters via Rotational Invariance Techniques – ESPRIT," in *Proc. Nineteenth Asilomar Conf. on Circuits, Systems and Comp.*, Asilomar, C.A., November 1985.
- [10] R. Schmidt, "Multiple emitter location and signal parameter estimation," in *Proceedings of RADC Spectrum Estimation Workshop*, 1979, pp. 243–258.
- [11] P. Stoica, P. Babu, and J. Li, "SPICE : a novel covariance-based sparse estimation method for array processing," *IEEE Trans. Signal Process.*, vol. 59, no. 2, pp. 629 –638, Feb. 2011.
- [12] J. F. Böhme, "Estimation of Spectral Parameters of Correlated Signals in Wavefields," *Signal Processing*, vol. 10, pp. 329–337, 1986.
- [13] P. Stoica and R. Moses, *Spectral Analysis of Signals*, Prentice Hall, Upper Saddle River, N.J., 2005.
- [14] U. Grenander and G. Szegö, *Toeplitz Forms and Their Applications*, University of California Press, Los Angeles, 1958.
- [15] A. G. Jaffer, "Maximum Likelihood Direction Finding of Stochastic Sources: A Separable Solution," in *13th IEEE Int. Conf. on Acoustics, Speech and Signal Processing*, New York, N.Y., 1988, pp. 2893–2896.
- [16] P. Stoica and A. Nehorai, "MUSIC, Maximum Likelihood, and Cramér-Rao Bound," *IEEE Trans. Acoust., Speech, Signal Process.*, vol. 37, no. 5, pp. 720–741, May 1989.
- [17] P. Stoica and A. Nehorai, "On the Concentrated Stochastic Likelihood Function in Array Signal Processing," *Circ. Syst. Signal Process.*, vol. 14, no. 5, pp. 669–674, 1995.
- [18] J-P. Delmas, "Asymptotic Normality of Sample Covariance Matrix for Mixed Spectra Time Series: Application to Sinusoidal Frequencies Estimation," *IEEE Trans. Inf. Theor.*, vol. 47, no. 4, pp. 1681–1687, 2001.
- [19] J-P. Delmas, "Asymptotic Performance of Second-Order Algorithms," *IEEE Trans. Signal Process.*, vol. 50, no. 1, pp. 49–57, 2002.
- [20] J-P. Delmas and Y. Meurisse, "Robustness of narrowband DOA algorithms with respect to signal bandwidth," *Signal Process.*, vol. 83, pp. 493–510, 2003.
- [21] J-P. Delmas and Y. Meurisse, "Asymptotically minimum variance second-order estimation for complex circular processes," *Signal Process.*, vol. 86, pp. 2289–2295, 2006.
- [22] A. Adler and M. Wax, "Direct Localization by Partly Calibrated Arrays: A Relaxed Maximum Likelihood Solution," in *27th European Signal Processing Conference*, A Coruna, Spain, 2019.
- [23] F. Elvander, R. Ali, A. Jakobsson, and T. van Waterschoot, "Offline Noise Reduction Using Optimal Mass Transport Induced Covariance Interpolation," in *Proc. 27th European Signal Process. Conf.*, A Coruna, Spain, Sept. 2019.
- [24] B. Ottersten, P. Stoica, and R. Roy, "Covariance matching estimation techniques for array signal processing applications," *Digit. Signal Process.*, vol. 8, pp. 185–210, 1998.
- [25] K. Hoffman, *Banach spaces of analytic functions*, Prentice-Hall series in modern analysis. Prentice-Hall, 1962.
- [26] V. Bentkus, "A Lyapunov-type bound in \mathbb{R}^d ," *Theory of Probability & Its Applications*, vol. 49, no. 2, pp. 311–323, 2005.
- [27] M. Raic, "A multivariate Berry-Esséen theorem with explicit constants," *arXiv:1802.06475*, 2018.